Fra-1 transgenic mouse as a model for systemic sclerosis: a potential role of M2 polarization

Journal:	*Journal of Scleroderma and Related Disorders*
Manuscript ID	JSO-18-0015.R1
Manuscript Type:	Original Manuscript
Keywords:	Interstitial lung disease, Macrophages, Mouse model, Pulmonary arterial hypertension, Systemic sclerosis
Abstract:	Objectives. To investigate the systemic sclerosis (SSc)-related phenotype in Fra-1 transgenic (tg) mice and its underlying mechanisms. Methods. Lung and skin sections of constitutive Fra-1 tg mice and wild-type (WT) mice were examined by tissue staining and immunohistochemistry. The tricuspid regurgitation pressure gradient (TRPG) was measured by transthoracic echocardiography with a Doppler technique. To assess the impact of Fra-1 expression on macrophage function, bone marrow-derived mononuclear cells (BMDCs) were derived from mice that expressed Fra-1 under the control of doxycycline and WT littermates. These BMDCs were induced to differentiate into macrophages with or without doxycycline, and analyzed for gene and protein expression. Finally, lung explants obtained from SSc patients and control donors were subjected to immunohistochemistry. Results. The lungs of Fra-1 tg mice showed excessive fibrosis of the interstitium and thickening of vessel walls, with narrowing lumen, in an age-dependent manner. The TRPG was significantly elevated in Fra-1 tg versus control mice. Increased dermal thickness and the loss of subdermal adipose tissue were also observed in the Fra-1 tg mice. These changes were preceded by a perivascular infiltration of mononuclear cells, predominantly consisting of alternatively activated or M2 macrophages. Overexpressing Fra-1 in BMDC cultures increased the expression of M2-related genes, such as Il10, Alox15, and Arg1. Finally, Fra-1-expressing M2 macrophages were increased in the lung tissues of SSc patients. Conclusions. The Fra-1 tg mouse serves as a genetic model of SSc that recapitulates the major vascular and fibrotic manifestations of the lungs and skin in SSc patients. M2 polarization mediated by the up-regulation of Fra-1 may play a critical role in the development of SSc.

Original Manuscript JSO-18-0015.R1

Fra-1 transgenic mouse as a model for systemic sclerosis: a potential role of M2 polarization

Hidekata Yasuoka[1], Yuen Yu Angela Tam[1], Yuka Okazaki[1,2], Yuichi Tamura[3], Koichi Matsuo[4], Carol Feghali-Bostwick[5], Tsutomu Takeuchi[1], and Masataka Kuwana[1,2]

[1]Division of Rheumatology, Department of Internal Medicine, Keio University School of Medicine, Tokyo, Japan; [2]Department of Allergy and Rheumatology, Nippon Medical School Graduate School of Medicine, Tokyo, Japan; [3]International University of Health and Welfare, Mita Hospital, Tokyo, Japan; [4]Laboratory of Cell and Tissue Biology, Keio University School of Medicine, Tokyo, Japan; and [5]Medical University of South Carolina, Charleston, South Carolina, United States.

Corresponding author: Masataka Kuwana, MD, PhD

Department of Allergy and Rheumatology, Nippon Medical School Graduate School of Medicine, 1-1-5 Sendagi, Bunkyo-ku, Tokyo 113-8603-8582, Japan

Phone: +81-3-3822-2131

Fax: +81-3-3815-3049

E-mail: kuwanam@nms.ac.jp

ABSTRACT

Objectives. To investigate the systemic sclerosis (SSc)-related phenotype in Fra-1 transgenic (tg) mice and its underlying mechanisms.

Methods. Lung and skin sections of constitutive Fra-1 tg mice and wild-type (WT) mice were examined by tissue staining and immunohistochemistry. The tricuspid regurgitation pressure gradient (TRPG) was measured by transthoracic echocardiography with a Doppler technique. To assess the impact of Fra-1 expression on macrophage function, bone marrow-derived mononuclear cells (BMDCs) were derived from mice that expressed Fra-1 under the control of doxycycline and WT littermates. These BMDCs were induced to differentiate into macrophages with or without doxycycline, and analyzed for gene and protein expression. Finally, lung explants obtained from SSc patients and control donors were subjected to immunohistochemistry.

Results. The lungs of Fra-1 tg mice showed excessive fibrosis of the interstitium and thickening of vessel walls, with narrowing lumen, in an age-dependent manner. The TRPG was significantly elevated in Fra-1 tg versus control mice. Increased dermal thickness and the loss of subdermal adipose tissue were also observed in the Fra-1 tg mice. These changes were preceded by a perivascular infiltration of mononuclear cells, predominantly consisting of alternatively activated or M2 macrophages. Overexpressing Fra-1 in BMDC cultures increased the expression of M2-related genes, such as *Il10*, *Alox15*, and *Arg1*. Finally, Fra-1-expressing M2 macrophages were increased in the lung tissues of SSc patients.

Conclusions. The Fra-1 tg mouse serves as a genetic model of SSc that recapitulates the major vascular and fibrotic manifestations of the lungs and skin in SSc patients. M2 polarization mediated by the up-regulation of Fra-1 may play a critical role in the development of SSc.

Keywords:

Interstitial lung disease, Macrophages, Mouse model, Pulmonary arterial hypertension, Systemic sclerosis

Introduction

Systemic sclerosis (SSc) is a connective tissue disease characterized by excessive fibrosis, widespread vasculopathy, and immune dysregulation [1]. An excessive and uncontrolled deposition of extracellular matrix (ECM) components, which causes a loss of function in various affected organ systems, is the end result of a complex series of interlinked vascular injuries and immune activations [2], although the complex interplay between vasculopathy, immune cell activations, and fibrosis in this disease is still incompletely understood. Animal models are valuable for elucidating the pathogenic mechanisms of a disease and for assessing therapeutic approaches before clinical trials, but there is currently no perfect animal model of SSc that fully recapitulates the features of the human disease [3].

The Fos-related antigen-2 (Fra-2) transgenic (tg) mouse is a genetic model of SSc that recapitulates the major vascular and fibrotic manifestations of the skin, lungs, and heart in SSc patients [4-7]. In the course of investigation into mechanisms regulating bone formation, one of the authors (KM) observed that mice that constitutively overexpressed another Fos-related antigen, Fra-1, also showed inflammation and progressive collagen deposition in the lungs. Fra-1 tg mice are known to exhibit a progressive increase in bone mass of the entire skeleton, leading to osteosclerosis [8]. Both Fra-1 and Fra-2 are members of the Fos protein family, which is a component of the transcription factor activator protein-1 (AP-1) and participates in a wide range of cellular processes, including proliferation, apoptosis, differentiation, survival, cell migration, and transformation [9]. AP-1 is composed of homodimers or heterodimers of the Fos, Jun, and activating transcription factor protein families, characterized as having a highly conserved dimeric basic leucine zipper DNA-binding domain [10]. AP-1 transcriptional regulation is involved in many pathologic cellular processes, including cancer, inflammation, and fibrosis [11, 12]. AP-1 also plays a prominent role in the ECM deposition in pathologic fibrosis settings, including SSc [13-16]. In this study, we assessed the detailed SSc phenotype of Fra-1 tg mice and investigated the mechanisms responsible for its SSc phenotype.

Methods

Patients

Lung explants were obtained from 5 SSc patients with interstitial lung disease (ILD) and/or pulmonary arterial hypertension (PAH) who underwent lung transplantation at the University of Pittsburgh Medical Center, as described previously [17]. All patients fulfilled the 2013 classification criteria for SSc proposed by the American College of Rheumatology/European League against Rheumatism [18]. Control lungs were obtained from 3 normal donor lungs that were not used for transplantation. All subjects signed a consent form approved by the University of Pittsburgh institutional review boards.

Fra-1 tg mice

We used two types of female Fra-1 tg mice: mice that constitutively expressed Fra-1 (constitutive Fra-1 tg mice) and mice that expressed inducible Fra-1 under the control of doxycycline (Dox) (Dox-inducible Fra-1 tg mice). These mice were generous gifts from Dr. Erwin F. Wagner, the Spanish National Cancer Research Center, Madrid, Spain. The transgene construct of the constitutive Fra-1 tg mouse was generated by fusing the full-length murine Fra-1 gene to the promotor of major histocompatibility complex class I antigen H2-K^b, to allow for the expression of Fra-1 in various cell types [8]. The Dox-inducible Fra-1 tg mice demonstrated a tight, Dox-dependent regulation of the ectopic Fra-1 gene expression [19]. Ectopic Fra-1 expression under the control of Dox was confirmed to be similar to that of the constitutive tg mice, and was efficiently shut down as early as 5 days after Dox removal. Wild-type littermates were used as controls for both types of Fra-1 tg mice. All animal experimental protocols were approved *a priori* by the Keio University Institutional Animal Care and Use Committee.

Histological analysis

Age-matched constitutive Fra-1 tg mice and wild-type littermates were sacrificed, and the skin, heart, and lung tissues were harvested and fixed in 10% buffered formalin or snap-

frozen in liquid nitrogen. In some instances, excised organs were macroscopically observed. The heart was cut in the short-axis plane, and the ratio of right-ventricle-wall thickening to left-ventricle-wall thickening plus septum thickening (RV/[LV+S]) was calculated as an indicator of right-ventricular hypertrophy, which is modified from Fulton's index [20]. Formalin-fixed, paraffin-embedded specimens cut into 3-5-μm sections were stained with hematoxylin and eosin or Masson's trichrome. The severity of lung fibrosis was semi-quantitatively assessed using the Ashcroft scoring system [21]. Dermal thickness was assessed in Masson's trichrome-stained skin sections [5]. The average of measurements from 10 randomly selected fields was used for each mouse.

For the immunostaining of tissue sections, aminoethyl carbazole (AEC) or fluorescent staining was performed as described previously [22, 23]. The primary antibodies used were anti-CD68 monoclonal antibody (mAb) (AbD Serotec, Raleigh, NC, USA) for the detection of macrophages, anti-CD3 mAb (Thermo Fisher Scientific, Waltham, MA, USA) for T cells, and anti-CD45R/B220 mAb (BD Biosciences, San Jose, CA, USA) for B cells. Anti-α-smooth muscle actin (αSMA) and anti-CD31 mAbs (Sigma-Aldrich, St Louis, MO, USA) were also used. Negative controls were cells incubated with isotype-matched Abs to an irrelevant antigen, instead of the primary antibody. Nuclei were counter-stained with hematoxylin. In some instances, consecutive frozen sections (10-μm thick) were used for fluorescent staining. To distinguish between "classically activated" or M1 macrophages and "alternatively activated" or M2 macrophages, mannose receptor C type I CD206 and arginase-1 (in mouse), class A scavenger receptor CD204 (in human) were used as M2 markers [24]. Specifically, the slides were incubated with an anti-CD68 mAb (AbD Serotec) and anti-CD206 polyclonal antibodies (Abcam, Cambridge, MA, USA) or anti-arginase-1 polyclonal antibodies (Santa Cruz Biotechnology, Dallas, TX, USA), with or without anti-Fra-1 polyclonal antibodies (Santa Cruz Biotechnology), followed by an incubation with AlexaFluor® 488 and AlexaFluor® 568 species-specific IgG (Thermo Fisher Scientific). For the staining of human samples, formalin-fixed, paraffin-embedded sections (6-μm thick) were incubated with an anti-CD68 mAb (Agilent Technologies Inc, Santa Clara, CA) and anti-CD204 polyclonal antibodies (TranGenic Inc, Fukuoka, Japan), with or without anti-Fra-1

antibody (Santa Cruz Biotechnology). Nuclei were counter-stained with TO-PRO3 (Life Technologies, Grand Island, NY, USA). The slides were examined with a confocal laser fluorescence microscope (Fluoview FV1000: Olympus, Tokyo, Japan). To determine the number of cells staining positive for a given marker, at least 10 fields per mouse were evaluated at high-power field (HPF; x400).

Trans-thoracic echocardiography

Mice were anesthetized by 1.5% isoflurane inhalation and were anchored to a platform in the supine position. Short axis echocardiography and Doppler echocardiographic measurements were made using the Vevo 660 system (VisualSonics, Toronto, Ontario, Canada) with a 600 series real-time microvisualization scanhead probe [25]. The velocity of tricuspid regurgitation jet was measured, and the tricuspid regurgitation pressure gradient (TRPG) was calculated based on a simplified Bernoulli equation. RV/(LV+S) was used to assess the degree of right ventricular hypertrophy.

***In vitro* induction of macrophages**

Macrophages were derived *in vitro* in cultures of bone marrow-derived cells (BMDCs) as described previously [26] with some modifications. In brief, bone marrow cells were isolated by flushing the femurs of Dox-inducible Fra-1 tg and control mice with phosphate buffered saline (PBS), and the BMDCs were purified by density gradient centrifugation using Lymphosepar II (ImmunoBiological Laboratories, Takasaki, Japan) at 400 g for 30 minutes. The buffy-coat layer was harvested and rinsed with PBS, and pelleted by centrifugation at 300 g for 10 minutes. The cells were resuspended in complete medium consisting of RPMI 1640, 4-[2-hydroxyethyl]-1-piperazineethanesulfonic acid (25 mM), L-glutamine (2 mM), 10% fetal bovine serum (FBS), penicillin (100 U/ml), and streptomycin (100 μg/ml) at 6 x 10^5 cells/mL, and cultured in 12-well plates with macrophage colony-stimulating factor (M-CSF) (100 U/mL) (Peprotech, Rocky Hill, NJ, USA), in the presence or absence of Dox (1 μg/mL) (Sigma-Aldrich). The medium was changed every 3 days to fresh medium containing the same supplements except that the FBS concentration was reduced to 0.1%. On day 7, the

adherent cells were harvested by incubating them with 2 mM ethylenediaminetetraacetic acid in PBS on ice for 30 minutes.

Semi-quantitative and quantitative polymerase-chain reaction (PCR)

The mRNA expression was examined using reverse transcription-PCR. Briefly, total RNA was isolated from cultured cells using an RNeasy MiniKit (Qiagen, Valencia, CA, USA) according to the manufacturer's protocol. One microgram of RNA was reverse transcribed into cDNA with oligo[dT]$_{12\text{-}18}$ primers (Takara Bio, Shiga, Japan), and subjected to PCR. The genes examined included the M1 markers *Tnfa* and *Il12;* M2 markers *Il10*, *Alox15*, *Fizz1*, and *Ym1* [27]; and an internal control *Beta-actin* (Supplemental Table). After amplification, the samples were separated by electrophoresis on a 2% agarose gel, and the bands were visualized with ethidium bromide. The intensities of the bands were quantified using Image J software (National Institute of Health, Bethesda, MA, USA) and normalized to that of *Beta-actin*. In some experiments, mRNA expression was quantitatively measured using TaqMan® real-time PCR system (Applied Biosystems, Foster City, CA, USA) using 18S rRNA for standardization. Specific primers and probes for type I collagen alpha 1 and 2 (*co1a1* and *col1a2*) were purchased from Applied Biosystems.

Quantification of collagen in lung tissue

The collagen deposition in lung tissue was analyzed quantitatively by Sircol collagen dye-binding assay (Biocolor, Newtownabbey, UK).

Detection of anti-nuclear antibody (ANA)

Indirect immunofluorescence was conducted using plasma diluted at 1:20 for detection of ANA using Fluoro HEPANA test (MBL, Nagoya, Japan), in which AlexaFluor® 488-conjugated anti-mouse IgG antibodies were used as secondary antibody.

Cytometric bead array

Cytokines and chemokines (IL-12p70, interferon [IFN]-γ, tumor necrosis factor [TNF]-α, IL-

10, CCL2, and IL-6) in macrophage culture supernatants were measured using a flow cytometry-based assay with the BD Cytometric bead array system (BD Biosciences) combined with a mouse inflammation kit. The cells were analyzed on a FACS® Calibur flow cytometer (BD Biosciences) using CellQuest software, according to the manufacturer's protocol.

Statistical analyses

The Mann-Whitney U test was used for unrelated, nonparametric samples. Data are expressed as the mean ± standard deviation. Values of $P < 0.05$ were considered statistically significant. Correlation was assessed using a single-regression model. All statistical analyses were performed using SPSS Statistics version 23 (IBM, Tokyo, Japan).

Results

Phenotype of the constitutive Fra-1 tg mice

The constitutive Fra-1 tg mice started to die after 9 weeks of age, and two thirds of them died within 18 weeks. The survival assessment of 11 pairs of tg and wild-type littermates showed that the survival of constitutive Fra-1 tg mice was significantly worse than that of wild-type ($P = 0.01$) (Supplemental Figure 1A). At 10 weeks of age, an enlarged cardiovascular system, including the lungs and heart, was easily visible macroscopically in the constitutive Fra-1 tg mice, compared with wild-type littermates (Supplemental Figure 1B), suggesting that the cardiopulmonary condition was involved in the increased mortality. We confirmed that Fra-1 protein was detected in the lungs of constitutive Fra-1 tg mice, but not wild-type mice, at 5 weeks using immunofluorescence (Supplemental Figure 1C). Interestingly, Fra-1 was preferentially expressed in infiltrating mononuclear cells, compared to other cell types residing in the lung, such as epithelial cells, endothelial cells, and fibroblasts, consistent with a previous report [28]. We further examined the phenotype of the constitutive Fra-1 tg mice, focusing on features recapitulating SSc organ involvement, including ILD, PAH, and skin sclerosis. ANA was detected in none of Fra-1 tg mice or wild-type littermates.

Pulmonary interstitium: We first evaluated the lung tissues of constitutive Fra-1 tg mice and their wild-type littermates at 10 weeks after birth (Figure 1A). Masson-trichrome staining showed an enlarged interstitium characterized by mononuclear infiltration and excessive fibrotic change in the Fra-1 tg mice. These interstitial changes were uniform, and were observed mainly within the alveolar septa and perivascular-bronchial bundles, while fibroblastic foci or cystic changes were not detected. These characteristics were consistent with the non-specific interstitial pneumonia that is often found in SSc patients [29]. Serial evaluations of the lung tissues of constitutive Fra-1 tg mice and their wild-type littermates are shown in Figure 1B. The interstitial changes had already started at 5 weeks, and gradually progressed over time. After 16 weeks of age, the majority of alveoli were collapsed and replaced by fibrotic tissue in the Fra-1 tg lung. The extent of lung fibrosis was semi-quantitatively assessed using the Ashcroft score, which was correlated with age ($r^2 = 0.87$, $P < 0.00003$) (Figure 1C). Collagen deposition was increased in Fra-1 tg mice compared with wild-type littermates (5.1 ± 0.6 versus 1.8 ± 1.4 μg/100 μg weight of lung tissue, $P < 0.05$). In addition, mRNA expression of *col1a1* and *col1a2* in the lung tissue was elevated in Fra-1 tg than in wild-type mice (2.3 ± 2.9 versus 1.0 ± 0.0, 19.1 ± 18.1 versus 1.0 ± 0.0, respectively, $P < 0.05$ for both comparisons).

Pulmonary vasculature*:* The pulmonary arteries of 10-week-old constitutive Fra-1 tg mice showed prominent thickening of the vessel walls and narrowing of the lumen, compared with their wild-type littermates (Figure 2A). As shown in Figure 2B, detailed examination of the vascular structure revealed a mixture of various degrees of vascular changes, including concentric laminar intimal thickening (a), medial hypertrophy (b), adventitial thickening with intimal and medial thickening (c), and concentric and eccentric non-laminar thickening (d), but no plexiform lesions, dilated/angiomatoid lesions, or vasculitis. These obstructive vascular changes were consistent with the histologic features of PAH in SSc patients [30]. Evaluation of the vasculature of constitutive Fra-1 tg and wild-type mice over time revealed significant perivascular mononuclear cell infiltrates in the Fra-1 tg mice at 5 weeks of age that

were gradually replaced by accumulated ECM (Figure 2C). Concentric laminar intimal thickening and medial hypertrophy became apparent at 10 weeks of age or later. Consecutive lung sections of 10-week-old constitutive Fra-1 tg mice showed that the thickened pulmonary arterial walls were composed mainly of accumulated ECM and α-SMA-positive cells, which were likely to be smooth muscle cells and myofibroblasts, while the endothelium was lined with a single layer of CD31-positive endothelial cells (Figure 2D). Finally, the neo-muscularization of arterioles, which was indicated by α-SMA staining, was specifically detected in lung tissues from Fra-1 tg mice at 10 weeks (Figure 2E).

To examine whether the histologic findings of pulmonary arterial narrowing resulted in functional consequences, trans-thoracic echocardiography was conducted in 4 pairs of 10-week-old constitutive Fra1 tg and wild-type mice. As shown in Supplemental Figure 2A, the tricuspid regurgitation jet was clearly visible in the Tra-1 tg mice, but not in wild-type mice, and the TRPG was significantly elevated in Fra-1 tg mice compared to their wild-type littermates (0.49 ± 0.37 versus 0.05 ± 0.03 mmHg, $P < 0.01$). In addition, the RV/[LV+S] was significantly greater in the Fra-1 tg mice than in the wild-type controls (0.40 ± 0.09 versus 0.12 ± 0.03, $P < 0.002$) (Supplemental Figure 2B). These findings indicated that the histologic features of the damaged pulmonary arteries were associated with a functional impairment of pulmonary circulation, consistent with PAH.

Skin: We examined the histology of the skin obtained from the back of 10-week-old constitutive Fra-1 tg and wild-type mice. Representative skin sections are shown in Figure 3A. Compared with the wild-type controls, the Fra-1 tg mice showed a thicker dermis, with increased perivascular mononuclear cell infiltrates and ECM accumulation. Notably, the subdermal adipose tissue was almost completely lost in the Fra-1 tg skin. Fra-1 tg mice showed a time-dependent increase in dermal thickness starting as early as 5 weeks. The dermis was significantly thicker in the constitutive Fra-1 tg mice compared to wild-type littermates (216 ± 26 versus 118 ± 22 μm, $P < 0.05$) (Figure 3B). These skin histologic features resemble the skin histology of SSc patients [31].

Evaluation of infiltrating mononuclear cells in the lungs of constitutive Fra-1 tg mice

The histologic features of the lungs and skin from constitutive Fra-1 tg mice began with infiltration of mononuclear cells, followed by the accumulation of ECM, and resultant structural remodeling. To identify the types of infiltrating mononuclear cells, we performed immunohistochemistry for macrophages, T cells, and B cells in the lung tissues from 4 pairs of Fra-1 tg and wild-type mice (Figure 4A and B). There were significantly more infiltrating macrophages in the constitutive Fra-1 tg than in wild-type lung (40 ± 10 versus 21 ± 7/HPF, $P < 0.05$), whereas there was no difference in the number of T or B cells. As shown in Figure 4C, virtually all of the macrophages in the lungs expressed Fra-1. There were significantly more CD206-positive M2 macrophages in the Fra-1 tg compared to wild-type mice (27 ± 10 versus 3 ± 1/HPF, $P < 0.05$), although the number of CD206-negative macrophages was comparable (11 ± 8 versus 16 ± 11/HPF). As a result, the M2/M1 ratio was significantly higher in the Fra-1 tg mice than in their wild-type littermates (4.7 ± 0.9 versus 0.2 ± 0.1, $P < 0.001$). Most of the macrophages infiltrating the lungs of the Fra-1 tg mice expressed M2-associated arginase-1 (Figure 4D). These findings collectively indicated that M2 polarization is a characteristic of the constitutive Fra-1 tg mice.

Role of the Fra-1 overexpression in M2 polarization

To examine whether the Fra-1 overexpression contributed to the promotion of M2 differentiation, we used Dox-inducible Fra-1 tg mice. BMDCs derived from the Dox-inducible Fra-1 tg and control mice were cultured under macrophage differentiation conditions in the presence or absence of Dox. The recovered macrophages were then subjected to gene expression analysis, and the culture supernatants were used to measure cytokines and chemokines. As shown in Figure 5A, significant increases in the gene expression of M2 markers *Il10*, *Alox15*, and *Arg1* were observed in the macrophages derived from the Dox-inducible Fra-1 tg mice in the presence versus the absence of Dox (1.60 ± 0.21 versus 0.50 ± 0.49; 0.59 ± 0.13 versus 0.11 ± 0.09; 0.31 ± 0.01 versus 0.12 ± 0.01, respectively, $P < 0.05$ for all comparisons), although there was no difference in the gene expression of the M1 markers *Tnfa* and *Il12*. Additional M2-related genes, including *Fizz1*

and *Ym1*, also exhibited a trend toward increased expression in the macrophages derived from Dox-inducible Fra-1 tg mice in the presence versus the absence of Dox. Finally, in the presence of Dox, the culture supernatants of macrophages derived from Dox-inducible Fra-1 tg mice contained more IL-10 than those derived from control mice (Figure 5B), but the levels of the M1-associated IL-12p70, IFN-γ, and TNF-α were comparable.

Fra-1 expression in infiltrating macrophages in lung tissues from SSc patients

Lung tissue sections obtained from 5 SSc patients with ILD or PAH and 3 healthy controls were immunostained for evaluation of Fra-1-expressing M2 macrophages. As shown in Figure 6A, Fra-1-expressing M2 macrophages, which were identified as cells expressing CD68 (blue), CD204 (green), and Fra-1 (red) simultaneously, were increased in the representative lung tissue from a patient with SSc, but not in the tissue from a healthy control. There were significantly more Fra-1-expressing M2 macrophages in lung tissues of SSc patients compared to donor controls (22 ± 4 versus 1 ± 1/HPF, $P < 0.05$) (Figure 6B).

Discussion

We demonstrated that Fra-1 tg mice spontaneously develop progressive fibrosis and occlusive vasculopathy of the lungs, leading to death by 18 weeks of age. These animals also develop progressive skin thickening. Thus, this animal model recapitulates the major vascular and fibrotic manifestations of the skin and lungs seen in SSc patients [4-7], and should be included in the genetic models of SSc, despite lack of autoantibody production. The phenotype of Fra-1 tg mice is principally similar to that of mice that constitutively expressing Fra-2, another Fos family protein [13-16].

In constitutive Fra-1 tg mice, the infiltration of macrophages, especially those with the M2 phenotype, into the lungs preceded vascular remodelling and the accumulation of ECM, which led to distortion of the organ structure. These observations suggest that the infiltration of M2 macrophages is critical for promoting the vascular remodelling and excessive fibrosis.

In this regard, accumulating evidence indicates that monocytes and macrophages have important roles in initiating and/or perpetuating the pathogenic process of SSc [24]. Specifically, the perivascular infiltration of macrophages has been detected in SSc skin, lung, and other tissues, especially in the early disease phase [32]. A variety of $CD14^+$ monocyte subpopulations are increased in the peripheral blood of SSc patients, including type I collagen-producing monocytes [33], $CXCR4^+$ circulating cells with monocytic and endothelial features [34], monocytic pro-angiogenic hematopoietic cells [35], monocytes expressing high levels of versican and CCL2 [36], and tissue inhibitor of metalloproteinases 1-expressing monocytes [37]. In addition, a recent study examining the lung tissue of SSc patients with ILD found prominent infiltrates of fibrocytes [38], which originated from precursors within the circulating $CD14^+$ monocytes [39]. Therefore, the pathogenic process of SSc is likely to be triggered by the recruitment of circulating monocytes to affected sites, where they acquire profibrotic properties, i.e., the production of a variety of profibrotic growth factors, cytokines, and chemokines, to stimulate resident mesenchymal cells, and their own trans-differentiation into ECM-producing cells [39-41].

In the Fra-1 tg mice, it is likely that M2 polarization contributes to the development of the SSc phenotype. Monocytes and macrophages were first reported to have a pivotal role in removing microbes by phagocytosis or by secreting cytokines, but recent studies have shown that their physiological and pathological roles are variable, leading to their classification into pro-inflammatory M1 and anti-inflammatory/pro-fibrotic M2 types [42-44]. Originally, M2 was implicated in the development of T helper 2 effector responses and in the suppression of M1 responses, but M2 activation also leads to the continuous production of pro-fibrotic mediators that promote myofibroblast proliferation and activation of the epithelial- or endothelial-mesenchymal transition, resulting in excessive fibrosis [43]. In addition, M2 regulates ECM turnover by modulating expression of matrix metalloproteinase (MMP) family members and the tissue inhibitors of MMPs [45]. Recently, the importance of M2 in the pathogenesis of SSc has been increasingly recognized. For example, it was shown that macrophages in the early SSc skin express M2 markers, including CD163 and CD204 [46]. In a phase II clinical trial of the anti-IL-6 receptor biologic tocilizumab in early, active patients

with diffuse cutaneous SSc, tocilizumab treatment resulted in the down-regulation of M2-associated genes in the skin, a sustained reduction in circulating CCL18, an M2-associated chemokine, and an improvement in skin sclerosis [47].

We clearly showed using Dox-inducible Fra-1 tg mice that overexpressing Fra-1 promotes M2 polarization. In this regard, in dextran sulfate sodium-induced colitis and bone fracture mouse models, macrophages overexpressing Fra-1 show an impaired production of pro-inflammatory cytokines, including TNF-α and IL-12, because Fra-1 is a negative regulator of NF-κB-mediated stress responses [48, 49]. Moreover, Fra-1 tg mice are sensitive to the diffuse lung injury induced by gefinitib combined with lipopolysaccharide, which is mediated through a massive accumulation of macrophages in association with the overproduction of several chemokines, including CCL2 [28]. Furthermore, a recent *in vitro* study reported that Fra-1 upregulation in RAW264.7 macrophages induces an M2 phenotype, which is characterized by the secretion of high levels of IL-10, CCL2, CCL22, and Arg-1 and decreased expressions of IL-12p35, TNF-α, and iNOS [50]. Taken together, these findings suggest that Fra-1 is an important inducer of M2 macrophages. Interestingly, CCL2, a soluble mediator that activates M2 macrophages, is a known target gene downstream of Fra-1 [28].

Previous studies [4, 8, 51, 52] and our report have indicated that broad expression of Fra-1 or Fra-2 in the constitutive transgenic mice show similar phenotype, including increased bone mass and generalized fibrosis, although direct comparison has never been conducted. Since, in Fra-1 tg mice, expression of other AP-1 components including Fra-2 was not altered [8], suggesting that expression of Fra-1 and Fra-2 is principally independent. The diverse cellular processes mediated by AP-1 family members in response to various physiological and pathogenic stimuli have generally been attributed to the nature of activation of Jun and Fos family members, their dimeric composition, and the duration of the subsequent induction of downstream genes [9, 10], however, the exact relevance of dimeric composition composed of either Fra-1 or Fra-2 to the cellular processes is largely undefined. Further studies to examine impact of Fra-1 and Fra-2 overexpression on AP-1 activity and resultant functional consequence in SSc phenotype is necessary.

A temporal relationship between cancer and SSc onset has been widely recognized,

especially in SSc patients with anti-RNA polymerase III antibodies [53]. Since AP-1 is involved also in the development, propagation, and invasion of cancer [9], Fra-1 tg mouse model might be useful for evaluating this connection. However, there was no tumor formation or production of SSc-related autoantibody in Fra-1 tg mice by age of SSc phenotype occurrence.

Conclusions

The Fra-1 tg mouse model is a new genetic model of SSc and recapitulates the major vascular and fibrotic manifestations of the skin and lungs in SSc patients. M2 polarization mediated by the up-regulation of Fra-1 may play a critical role in the development of the SSc phenotype. The use of this animal model will help clarify the roles of M2 macrophages in the pathogenesis of SSc.

Acknowledgements

We thank Drs. Yasunari Takada and Ichiro Takada, and Ms. Mari Fujiwara for their assistance with the mouse experiments. We also thank Dr. Hiroshi Takei for assistance in Sircol assay.

Disclosures

Financial support: This project was supported by funding from the Kan Research Institute, Inc, and from a research grant for intractable diseases from the Japanese Ministry of Health, Labour and Welfare.

Conflict of interest: All authors state that they have nothing to declare.

References

1. Varga J, Trojanowska M, Kuwana M. Pathogenesis of systemic sclerosis: recent insights of molecular and cellular mechanisms and therapeutic opportunities. J Scleroderma Relat Disord. 2017;2:137-152.
2. Bhattacharyya S, Wei J, Varga J. Understanding fibrosis in systemic sclerosis: shifting paradigms, emerging opportunities. Nat Rev Rheumatol. 2012;8:42-54.
3. Soare A, Ramming A, Avouac J, Distler JHW. Updates on animal models of systemic sclerosis. J Scleroderma Relat Disord. 2016;1:266-276.
4. Eferl R, Hasselblatt P, Rath M, et al. Development of pulmonary fibrosis through a pathway involving the transcription factor Fra-2/AP-1. Proc Natl Acad Sci USA. 2008;105:10525-10530.
5. Maurer B, Busch N, Jüngel A, et al. Transcription factor fos-related antigen-2 induces progressive peripheral vasculopathy in mice closely resembling human systemic sclerosis. Circulation. 2009;120:2367-2376.
6. Maurer B, Reich N, Juengel A, et al. Fra-2 transgenic mice as a novel model of pulmonary hypertension associated with systemic sclerosis. Ann Rheum Dis. 2012;71:1382-1387.
7. Venalis P, Kumánovics G, Schulze-Koops H, et al. Cardiomyopathy in murine models of systemic sclerosis. Arthritis Rheum. 2015;67:508-516.
8. Jochum W, David JP, Elliott C, et al. Increased bone formation and osteosclerosis in mice overexpressing the transcription factor Fra-1. Nat Med. 2000;6:980-984.
9. Eferl R, Wagner EF. AP-1: a double-edged sword in tumorigenesis. Nat Rev Cancer. 2003;3:859-868.
10. Hess J, Angel P, Schorpp-Kistner M. AP-1 subunits: quarrel and harmony among siblings. J Cell Sci. 2004;117:5965–5973.
11. Zenz R, Eferl R, Scheinecker C, et al. Activator protein 1 (Fos/Jun) functions in inflammatory bone and skin disease. Arthritis Res Ther. 2008;10:201.
12. Trop-Steinberg S, Azar Y. AP-1 expression and its clinical relevance in immune

disorders and cancer. Am J Med Sci. 2017;353:474-483.

13. Smart DE, Vincent KJ, Arthur MJ, et al. JunD regulates transcription of the tissue inhibitor of metalloproteinases-1 and interleukin-6 genes in activated hepatic stellate cells. J Biol Chem. 2001;276:24414-24421.
14. Reich N, Maurer B, Akhmetshina A, et al. The transcription factor Fra-2 regulates the production of extracellular matrix in systemic sclerosis. Arthritis Rheum. 2010;62:280-290.
15. Palumbo K, Zerr P, Tomcik M, et al. The transcription factor JunD mediates transforming growth factor β-induced fibroblast activation and fibrosis in systemic sclerosis. Ann Rheum Dis. 2011;70:1320-1326.
16. Avouac J, Palumbo K, Tomcik M, et al. Inhibition of activator protein 1 signaling abrogates transforming growth factor β-mediated activation of fibroblasts and prevents experimental fibrosis. Arthritis Rheum. 2012;64:1642-1652.
17. Pilewski JM, Liu L, Henry AC, et al. Insulin-like growth factor binding proteins 3 and 5 are overexpressed in idiopathic pulmonary fibrosis and contribute to extracellular matrix deposition. Am J Pathol. 2005;166:399-407.
18. van den Hoogen F, Khanna D, Fransen J, et al. 2013 classification criteria for systemic sclerosis: an American College of Rheumatology/European League against Rheumatism collaborative initiative. Arthritis Rheum. 2013;65:2734-2747.
19. Hasenfuss SC, Bakiri L, Thomsen MK, Hamacher R, Wagner EF. Activator protein 1 transcription factor Fos-related antigen 1 (Fra-1) is dispensable for murine liver fibrosis, but modulates xenobiotic metabolism. Hepatology. 2014;59:261-273.
20. Fulton RM, Hutchinson EC, Jones AM. Ventricular weight in cardiac hypertrophy. Br Heart J. 1952;14:413-420.
21. Ashcroft T, Simpson JM, Timbrell V. Simple methods of estimating severity of pulmonary fibrosis on a numerical scale. J Clin Pathol. 1988;41:467-470.
22. Kuwana M, Okazaki Y, Kodama H, et al. Endothelial differentiation potential of human monocyte-derived multipotential cells. Stem Cells. 2006;24:2733-2743.
23. Yasuoka H, Zhou Z, Pilewski JM, et al. Insulin-like growth factor-binding protein-5

induces pulmonary fibrosis and triggers mononuclear cellular infiltration. Am J Pathol. 2006;169:1633-1642.

24. Stifano G, Christmann RB. Macrophage involvement in systemic sclerosis: Do we need more evidence? Curr Rheumatol Rep. 2016;18:2.
25. Endo J, Sano M, Katayama T, et al. Metabolic remodelling induced by mitochondrial aldehyde stress stimulates tolerances to oxidative stress in the heart. Circ Res. 2009;105:1118-1127.
26. Wang YC, He F, Feng F, et al. Notch signaling determines the M1 versus M2 polarization of macrophages in antitumor immune responses. Cancer Res. 2010;70:4840-4849.
27. Gensel JC, Zhang B. Macrophage activation and its role in repair and pathology after spinal cord injury. Brain Res. 2015;1619:1-11.
28. Takada Y, Gresh L, Bozec A, et al. Interstitial lung disease induced by gefitinib and Toll-like receptor ligands is mediated by Fra-1. Oncogene. 2011;30:3821-3832.
29. Bouros D, Wells AU, Nicholson AG, et al. Histopathologic subsets of fibrosing alveolitis in patients with systemic sclerosis and their relationship to outcome. Am J Respir Crit Care Med. 2002;165:1581-1586.
30. Overbeek MJ, Vonk MC, Boonstra A, et al. Pulmonary arterial hypertension in limited cutaneous systemic sclerosis: a distinctive vasculopathy. Eur Respir J. 2009;34:371-379.
31. Rooper LM, Askin FB. Pathology of systemic sclerosis. In “Scleroderma -From Pathogenesis to Comprehensive Management”. Second edition. Edited by Varga J, et al: Springer, New York, USA. 2017:pp141-159.
32. Kraaling BM, Maul GG, Jimenez SA. Mononuclear cellular infiltrates in clinically involved skin from patients with systemic sclerosis of recent onset predominantly consist of monocytes/macrophages. Pathobiology. 1995;63:48-56.
33. Mathai SK, Gluati M, Peng X, et al. Circulating monocytes from systemic sclerosis patients with interstitial lung disease shown an enhanced profibrotic phenotype. Lab Invest. 2010;90:812-823.
34. Campioni D, Lo Monaco A, Lanza F, et al. $CXCR4^{+}$ circulating progenitor cells

coexpressing monocytic and endothelial markers correlating with fibrotic clinical features are present in the peripheral blood of patients affected by systemic sclerosis. Haematologica. 2008;93:1233-1237.

35. Yamaguchi Y, Okazaki Y, Seta N, et al. Enhanced angiogenic potency of monocytic endothelial progenitor cells in patients with systemic sclerosis. Arthritis Res Ther. 2010;12:R205.
36. Masuda A, Yasuoka H, Satoh T, Okazaki Y, Yamaguchi Y, Kuwana M. Versican is upregulated in circulating monocytes in patients with systemic sclerosis and amplifies a CCL2-mediated pathogenic loop. Arthritis Res Ther. 2013;15: R74.
37. Ciechomska M, Huigens CA, Hugle T, et al. Toll-like receptor-mediated, enhanced production of profibrotic TIMP-1 in monocytes from patients with systemic sclerosis: role of serum factors. Ann Rheum Dis. 2013;72:1382-1389.
38. Tourkina E, Bonner M, Oates J, et al. Altered monocyte and fibrocyte phenotype and function in scleroderma interstitial lung disease: reversal by caveolin-1 scaffolding domain peptide. Fibrogenesis Tissue Repair. 2011;4:15.
39. Abe R, Donnelly SC, Peng T, Bucala R, Metz CN. Peripheral blood fibrocytes: differentiation pathway and migration to wound sites. J Immunol. 2001;166:7556-7562.
40. Kuwana M, Okazaki Y, Kodama H, et al. Human circulating $CD14^+$ monocytes as a source of progenitors that exhibit mesenchymal cell differentiation. J Leukoc Biol 2003;74:833-845.
41. Binai N, O'Reilly S, Griffiths B, van Laar JM, Hügle T. Differentiation potential of $CD14^+$ monocytes into myofibroblasts in patients with systemic sclerosis. PLoS One. 2012;7:e33508.
42. Gordon S, Martinez FO. Alternative activation of macrophages: mechanism and functions. Immunity. 2010;32:593-604.
43. Braga TT, Agudelo JS, Camara NO. Macrophages during the fibrotic process: M2 as friend and foe. Front Immunol. 2015;6:602.
44. Martinez FO, Gordon S. The M1 and M2 paradigm of macrophage activation: time for reassessment. F1000Prime Rep. 2014;6:13.

45. Vinnakota K, Zhang Y, Selvanesan BC, Topi G, Salim T, Sand-Dejmek J, Jönsson G, Sjölander A. M2-like macrophages induce colon cancer cell invasion via matrix metalloproteinases. J Cell Physiol. 2017;232:3468-3480.
46. Higashi-Kuwata N, Jinnin M, Makino T, et al. Characterization of monocyte/macrophage subsets in the skin and peripheral blood derived from patients with systemic sclerosis. Arthritis Res Ther. 2010;12:R128.
47. Khanna D, Denton CP, Jahreis A, et al. Safety and efficacy of subcutaneous tocilizumab in adults with systemic sclerosis (faSScinate): a phase 2, randomised, controlled trial. Lancet. 2016;387:2630-2640.
48. Takada Y, Ray N, Ikeda E, et al. Fos proteins suppress dextran sulfate sodium-induced colitis through inhibition of NF-kB. J Immunol. 2010;184:1014-1021.
49. Yamaguchi T, Takada Y, Maruyama K, et al. Fra-1/AP-1 impairs inflammatory responses and chondrogenesis in fracture healing. J Bone Miner Res. 2009;24:2056-2065.
50. Wang Q, Ni H, Lan L, Wei X, Xiang R, Wang Y. Fra-1 protooncogene regulates IL-6 expression in macrophages and promotes the generation of M2d macrophages. Cell Res. 2010; 20:701-712.
51. Bozec A, Bakiri L, Jimenez M, Schinke T, Amling M, Wagner EF. Fra-2/AP-1 controls bone formation by regulating osteoblast differentiation and collagen production. J Cell Biol. 2010;190:1093-1106.
52. Kireva T, Erhardt A, Tiegs G, et al. Transcription factor Fra-1 induces cholangitis and liver fibrosis. Hepatology. 2011;53:1259-1269.
53. Shah AA, Casciola-Rosen L. Mechanistic and clinical insights at the scleroderma-cancer interface. J Scleroderma Relat Disord 2017;2:153-159.

Figure legends

Figure 1. Pulmonary interstitium of constitutive Fra-1 transgenic (tg) mice

(A) Representative images of Masson's trichrome-stained lung tissue obtained from constitutive Fra-1 tg and wild-type (WT) mice at 10 weeks of age. Bar denotes 1 mm. (B) Serial changes in Masson's trichrome-stained lung tissue from constitutive Fra-1 tg and WT mice. Representative images are shown. Bar denotes 1 mm. (C) Correlation between Ashcroft score and age in 9 Fra-1 tg mice.

Figure 2. Pulmonary vasculature of constitutive Fra-1 transgenic (tg) mice

(A) Representative images of pulmonary arteries in lung tissue from Fra-1 tg and wild-type (WT) mice at 10 weeks of age. Tissue sections were subjected to Masson's trichrome staining. Bar denotes 200 μm. (B) Characteristic histologic findings of pulmonary arteries in 10-week-old Fra-1 tg mice, including concentric laminar intimal thickening (a), medial hypertrophy (b), adventitial thickening (c), and concentric and eccentric non-laminar thickening (d). Lung tissues were stained with Masson's trichrome. Each bar denotes 100 μm. (C) Serial changes in Elastica van Gieson-stained lung tissue from constitutive Fra-1 tg and WT mice. Representative images of pulmonary arteries are shown. Bar denotes 100 μm. (D) Serial lung sections from 10-week-old Fra-1 tg and WT mice, stained with Elastica van Gieson (EVG), Masson's trichrome (MT), anti-αSMA, or anti-CD31. Representative images of similar findings obtained from 4 pairs of tg and WT mice are shown. Bar denotes 100 μm. (E) Representative findings of the neo-muscularization of arterioles (detected by αSMA staining, arrows) in lung tissue from 10-week-old Fra-1 tg mice. Representative images of similar findings obtained from 4 pairs of tg and WT mice are shown. Bars denote 1 mm (left) and 100 μm (right), respectively.

Figure 3. Skin of constitutive Fra-1 transgenic (tg) mice

(A) Representative images of skin sections from 10-week-old Fra-1 tg mice and wild-type (WT) littermates. Sections were stained with hematoxylin and eosin or Masson's trichrome.

Double-headed arrows indicate the thickness of the dermis. Scale bar denotes 100 μm. (B) Dermal thickness in Fra-1 tg and WT mice. Statistical comparison was made using the Mann-Whitney U-test.

Figure 4. Evaluation of infiltrated mononuclear cells in the lungs of constitutive Fra-1 transgenic (tg) mice

(A) Lung sections from Fra-1 tg and wild-type (WT) mice were stained for CD68 (macrophages), CD3 (T cells), and B220 (B cells). Bar denotes 100 μm. (B) The number of infiltrating macrophages, T cells, and B cells in 4 pairs of Fra-1 tg and WT mice. Results are shown as cells per high power field (HPF). Statistical comparisons were made using the Mann-Whitney U-test. (C) Detection of M2 macrophages in the lungs from Fra-1 tg and WT mice, determined by the co-expression of CD68 (green), CD206 (blue), and Fra-1 (red). Representative images of similar findings obtained from 4 pairs of tg and WT mice are shown. Bar denotes 100 μm. (D) Detection of M2 macrophages in the lungs from Fra-1 tg and WT mice, determined by examining the co-expression of CD68 (red), arginase-1 (Arg1, green), and TO-PRO3 (blue). Representative images of similar findings obtained from 4 pairs of tg and WT mice are shown. Bar denotes 100 μm.

Figure 5. Role of Fra-1 up-regulation in M2 polarization determined by *in vitro* culture of bone marrow-derived mononuclear cells (BMDCs)

BMDCs derived from doxycycline (Dox)-inducible Fra-1 transgenic (tg) and control mice were cultured under macrophage-differentiation conditions in the presence or absence of Dox. Four pairs of tg and WT mice were used. (A) Expression levels of genes associated with M1 and M2 macrophages in BMDCs from 4 pairs of Dox-inducible Fra-1 tg and control mice cultured in the presence or absence of Dox. Gene expression levels were detected by semi-quantitative polymerase chain reaction (PCR). *$P < 0.05$ by Mann-Whitney U-test. (B) Expression levels of cytokines and chemokines associated with M1 or M2 macrophages in the culture supernatants of BMDCs derived from Dox-inducible Fra-1 tg and control mice cultured under macrophage-differentiation conditions in the presence of Dox. Statistical

comparison was made using the Mann-Whitney U-test.

Figure 6. Fra-1 expression in infiltrated macrophages in the lung tissue from SSc patients with interstitial lung disease and/or pulmonary arterial hypertension

(A) Representative images of lung-tissue sections from a patient with SSc and a healthy control, stained for CD68 (blue), CD204 (green), and Fra-1 (red). Bar denotes 100 μm. (B) The number of cells positive for CD68, CD204, and Fra-1 in 5 patients with SSc and 3 healthy controls (HC). Results are shown as cells per high power field (HPF). Statistical comparisons were made using the Mann-Whitney U-test.

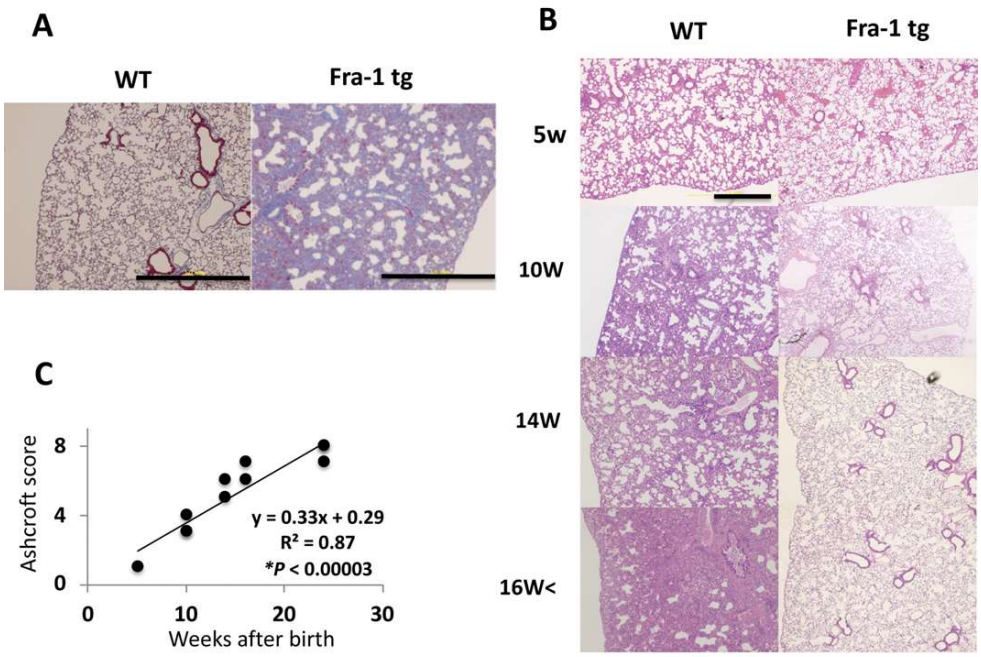

Figure 1. Pulmonary interstitium of constitutive Fra-1 transgenic (tg) mice
(A) Representative images of Masson's trichrome-stained lung tissue obtained from constitutive Fra-1 tg and wild-type (WT) mice at 10 weeks of age. Bar denotes 1 mm. (B) Serial changes in Masson's trichrome-stained lung tissue from constitutive Fra-1 tg and WT mice. Representative images are shown. Bar denotes 1 mm. (C) Correlation between Ashcroft score and age in 9 Fra-1 tg mice.

90x62mm (300 x 300 DPI)

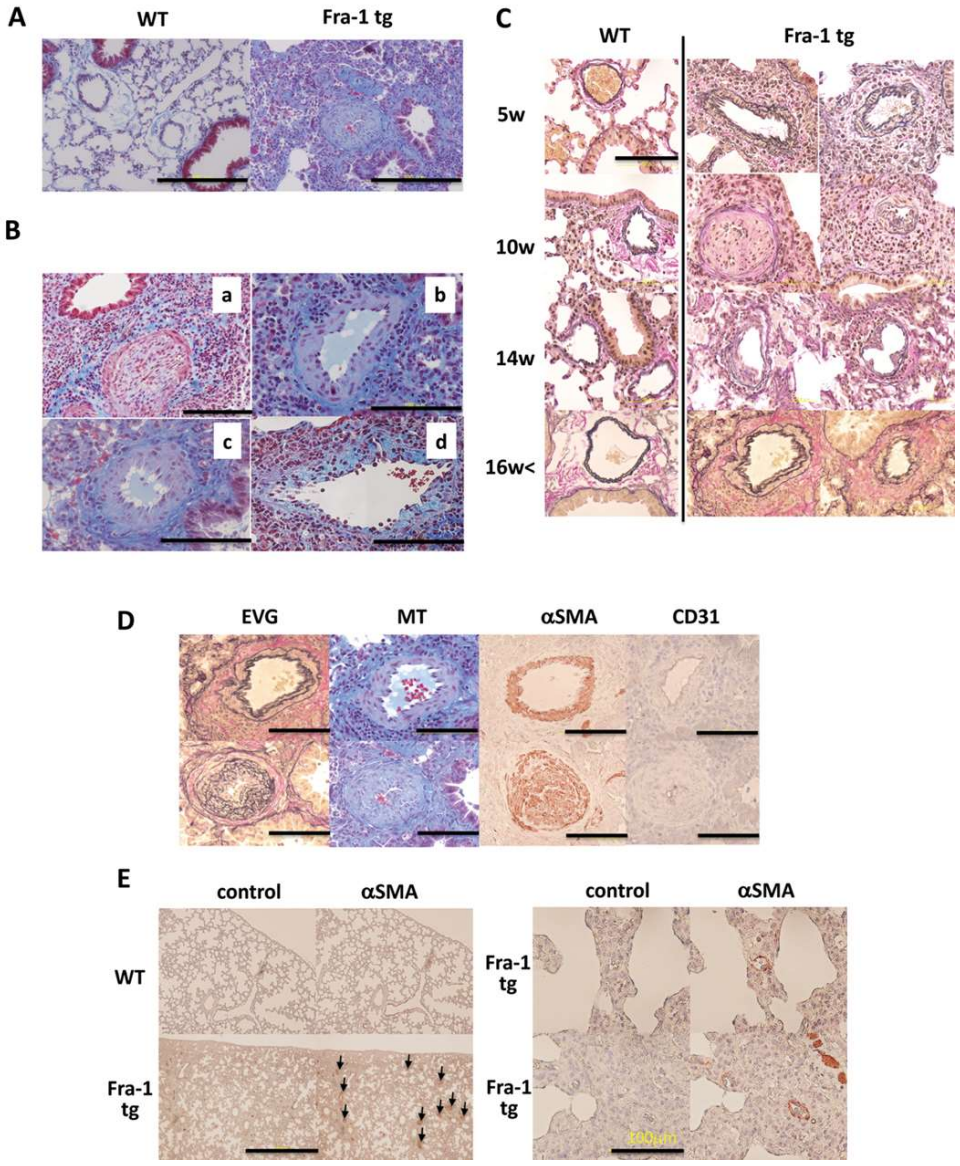

Figure 2. Pulmonary vasculature of constitutive Fra-1 transgenic (tg) mice
(A) Representative images of pulmonary arteries in lung tissue from Fra-1 tg and wild-type (WT) mice at 10 weeks of age. Tissue sections were subjected to Masson's trichrome staining. Bar denotes 200 μm. (B) Characteristic histologic findings of pulmonary arteries in 10-week-old Fra-1 tg mice, including concentric laminar intimal thickening (a), medial hypertrophy (b), adventitial thickening (c), and concentric and eccentric non-laminar thickening (d). Lung tissues were stained with Masson's trichrome. Each bar denotes 100 μm. (C) Serial changes in Elastica van Gieson-stained lung tissue from constitutive Fra-1 tg and WT mice. Representative images of pulmonary arteries are shown. Bar denotes 100 μm. (D) Serial lung sections from 10-week-old Fra-1 tg and WT mice, stained with Elastica van Gieson (EVG), Masson's trichrome (MT), anti-αSMA, or anti-CD31. Representative images of similar findings obtained from 4 pairs of tg and WT mice are shown. Bar denotes 100 μm. (E) Representative findings of the neo-muscularization of arterioles (detected by αSMA staining, arrows) in lung tissue from 10-week-old Fra-1 tg mice. Representative images of similar findings obtained from 4 pairs of tg and WT mice are shown. Bars denote 1 mm (left) and 100 μm (right), respectively.

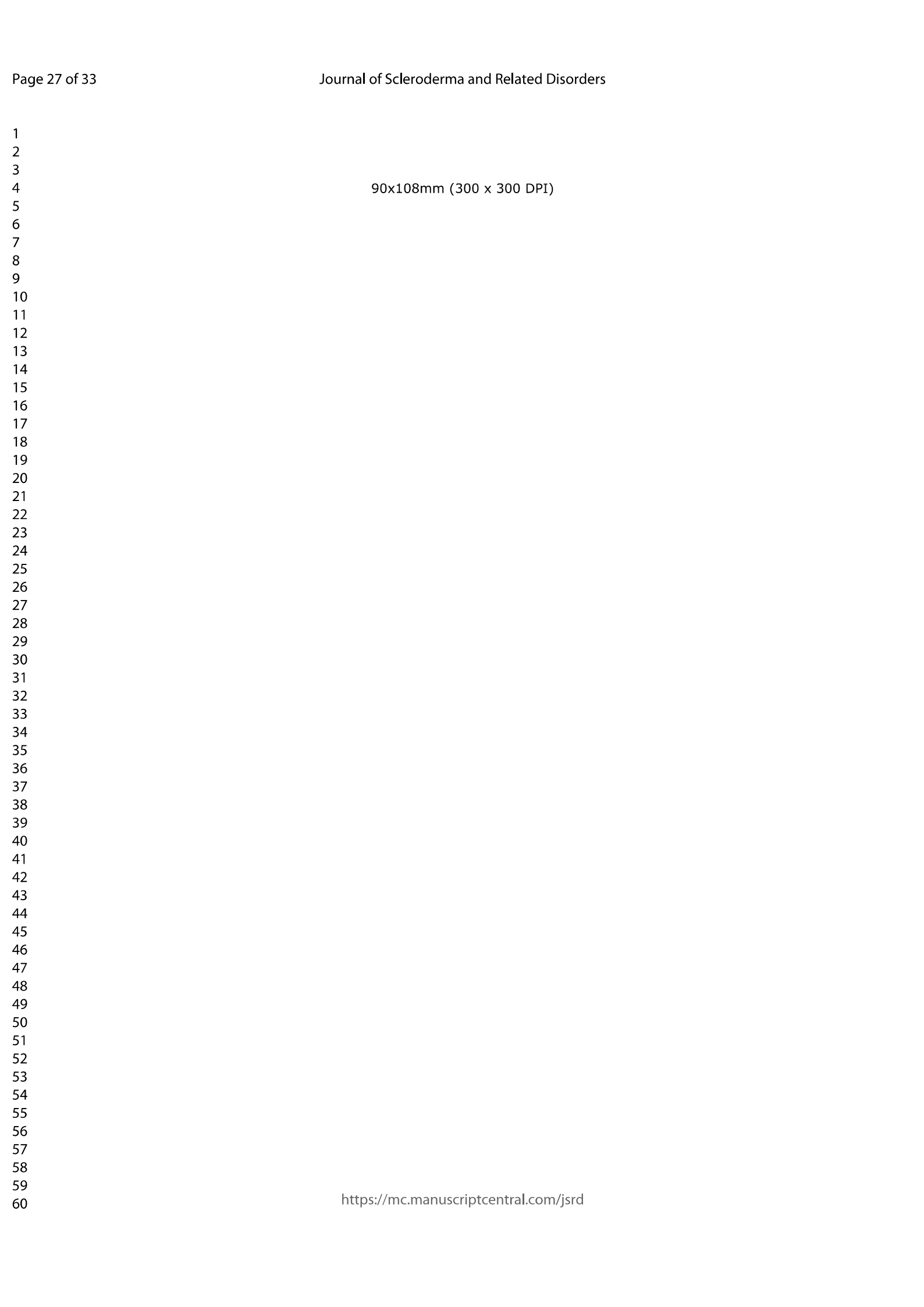
90x108mm (300 x 300 DPI)

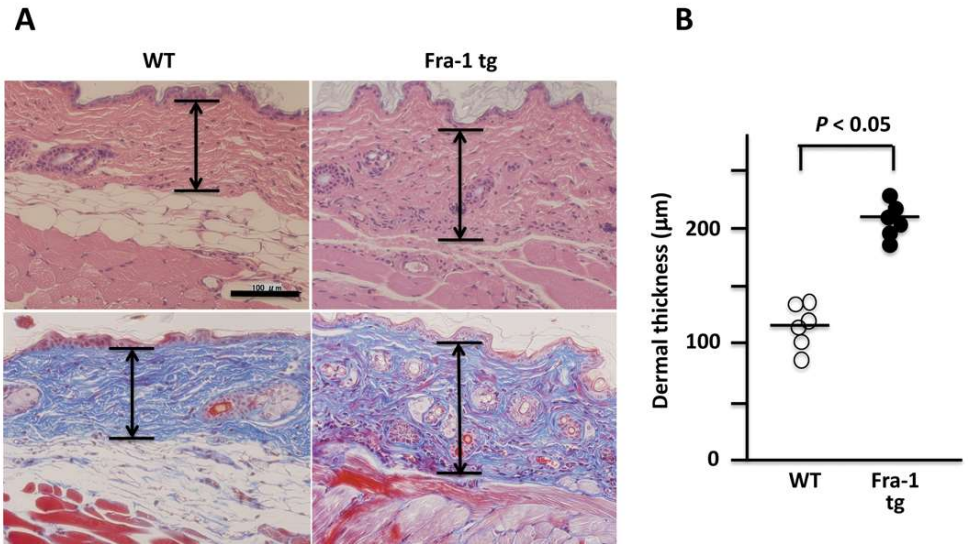

Figure 3. Skin of constitutive Fra-1 transgenic (tg) mice
(A) Representative images of skin sections from 10-week-old Fra-1 tg mice and wild-type (WT) littermates. Sections were stained with hematoxylin and eosin or Masson's trichrome. Double-headed arrows indicate the thickness of the dermis. Scale bar denotes 100 μm. (B) Dermal thickness in Fra-1 tg and WT mice. Statistical comparison was made using the Mann-Whitney U-test.

90x51mm (300 x 300 DPI)

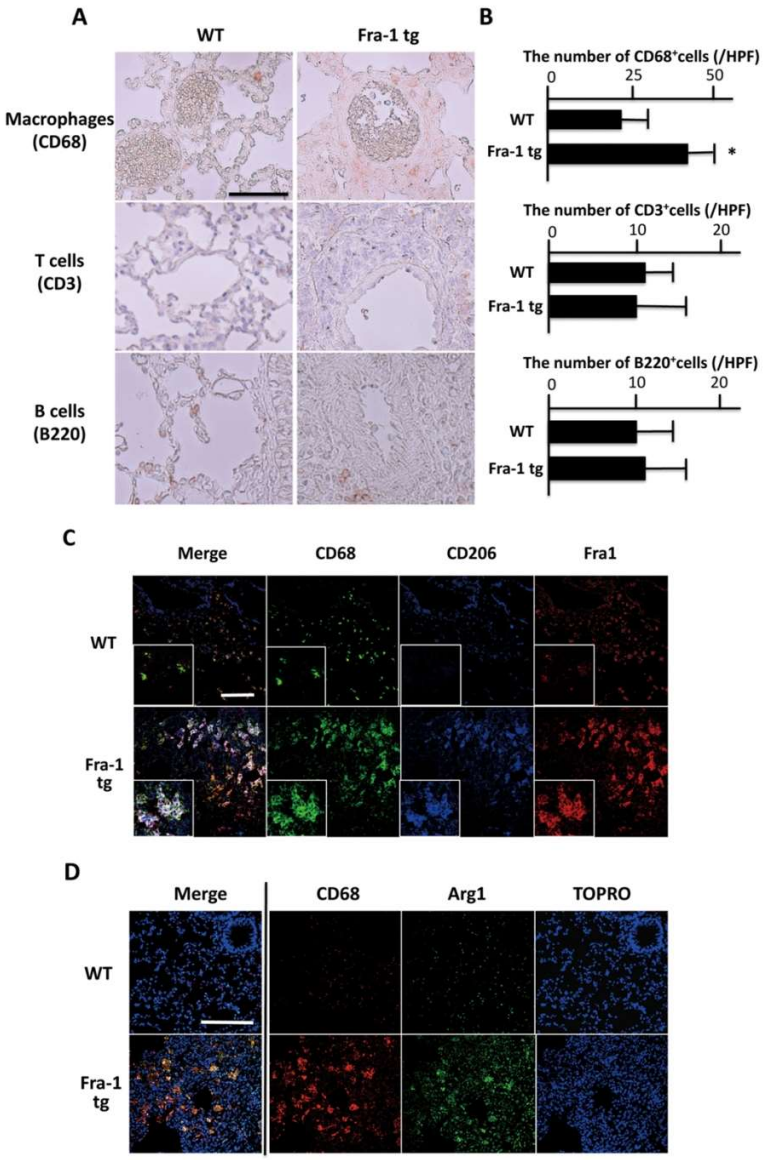

Figure 4. Evaluation of infiltrated mononuclear cells in the lungs of constitutive Fra-1 transgenic (tg) mice (A) Lung sections from Fra-1 tg and wild-type (WT) mice were stained for CD68 (macrophages), CD3 (T cells), and B220 (B cells). Bar denotes 100 μm. (B) The number of infiltrating macrophages, T cells, and B cells in 4 pairs of Fra-1 tg and WT mice. Results are shown as cells per high power field (HPF). Statistical comparisons were made using the Mann-Whitney U-test. (C) Detection of M2 macrophages in the lungs from Fra-1 tg and WT mice, determined by the co-expression of CD68 (green), CD206 (blue), and Fra-1 (red). Representative images of similar findings obtained from 4 pairs of tg and WT mice are shown. Bar denotes 100 μm. (D) Detection of M2 macrophages in the lungs from Fra-1 tg and WT mice, determined by examining the co-expression of CD68 (red), arginase-1 (Arg1, green), and TO-PRO3 (blue). Representative images of similar findings obtained from 4 pairs of tg and WT mice are shown. Bar denotes 100 μm.

90x135mm (300 x 300 DPI)

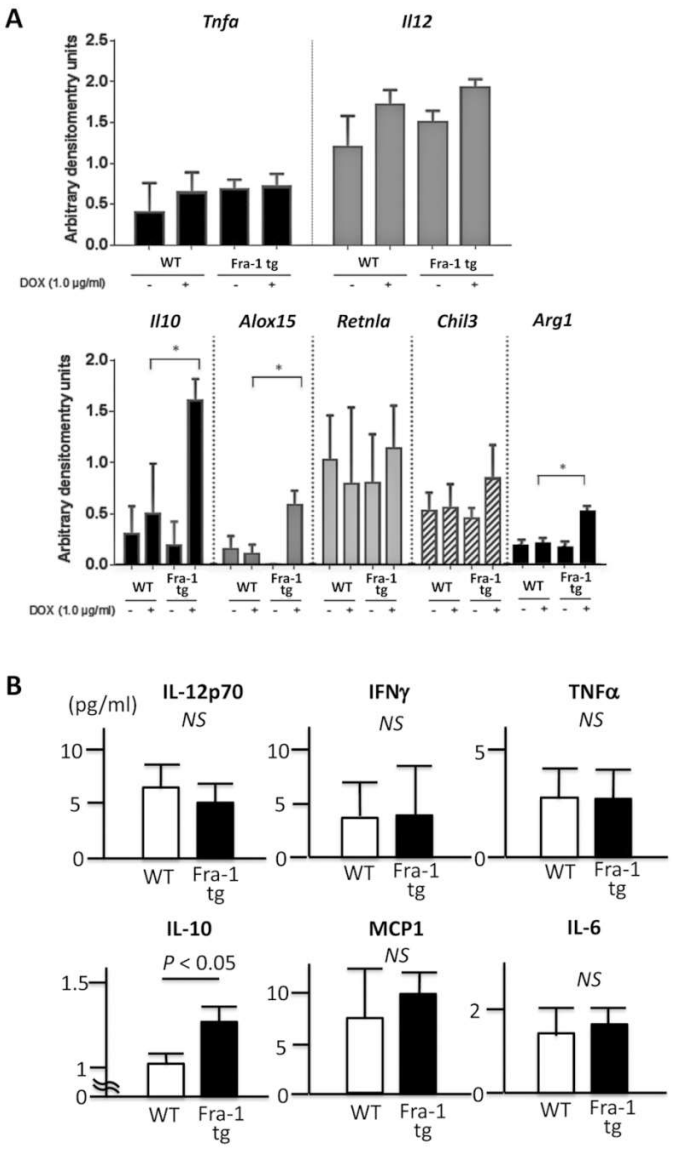

Figure 5. Role of Fra-1 up-regulation in M2 polarization determined by in vitro culture of bone marrow-derived mononuclear cells (BMDCs)

BMDCs derived from doxycycline (Dox)-inducible Fra-1 transgenic (tg) and control mice were cultured under macrophage-differentiation conditions in the presence or absence of Dox. Four pairs of tg and WT mice were used. (A) Expression levels of genes associated with M1 and M2 macrophages in BMDCs from 4 pairs of Dox-inducible Fra-1 tg and control mice cultured in the presence or absence of Dox. Gene expression levels were detected by semi-quantitative polymerase chain reaction (PCR). *P < 0.05 by Mann-Whitney U-test. (B) Expression levels of cytokines and chemokines associated with M1 or M2 macrophages in the culture supernatants of BMDCs derived from Dox-inducible Fra-1 tg and control mice cultured under macrophage-differentiation conditions in the presence of Dox. Statistical comparison was made using the Mann-Whitney U-test.

80x136mm (300 x 300 DPI)

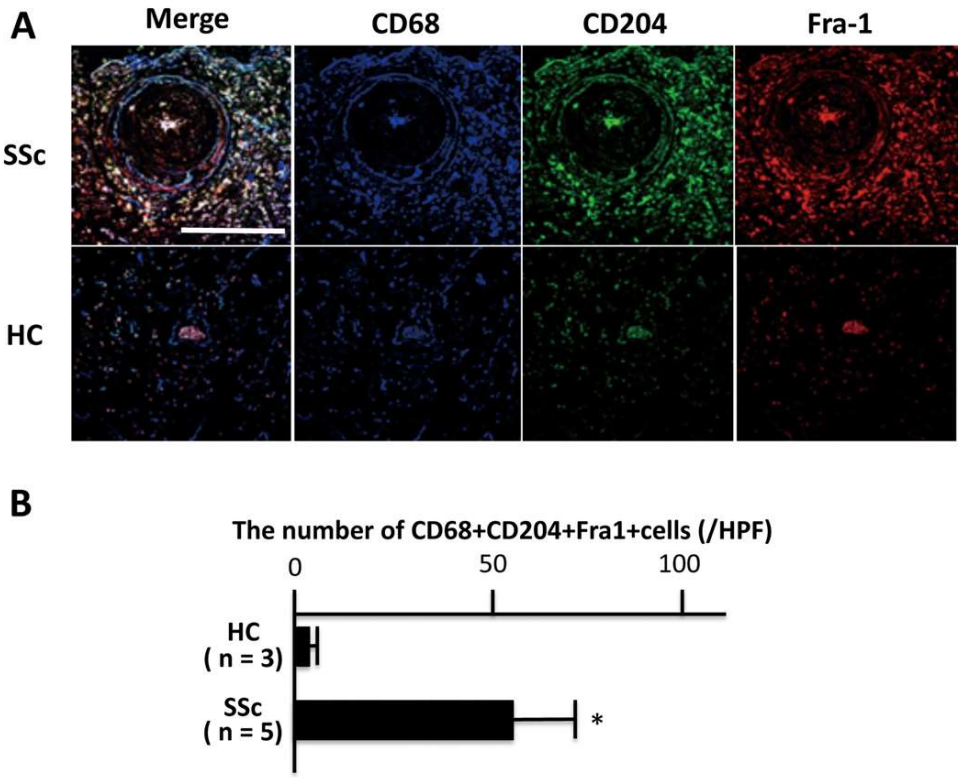

Figure 6. Fra-1 expression in infiltrated macrophages in the lung tissue from SSc patients with interstitial lung disease and/or pulmonary arterial hypertension
(A) Representative images of lung-tissue sections from a patient with SSc and a healthy control, stained for CD68 (blue), CD204 (green), and Fra-1 (red). Bar denotes 100 μm. (B) The number of cells positive for CD68, CD204, and Fra-1 in 5 patients with SSc and 3 healthy controls (HC). Results are shown as cells per high power field (HPF). Statistical comparisons were made using the Mann-Whitney U-test.

90x73mm (300 x 300 DPI)

Supplemental Table. Primer sets for semi-quantitative PCR

Category	Gene name	Sense (5' → 3')	Antisense (5' → 3')
M1-related	*Tnfa*	CCTGTAGCCCACGTCGTAGC	AGCAATGACTCCAAAGTAGACC
	Il12	CAGAAGCTAACCATCTCCTGGTTTG	TCCGGAGTAATTTGGTGCTTCACAC
M2-related	*Il10*	CTATGCTGCCTGCTCTTACTG	GATGGCCTTGTAGACACCTTGG
	Alox15	CAGCTGGATTGGTTCTACTG	CTCTGAACTTCTTCAGCACAG
	Fizz1	CCCAGTGAATACTGATGAGACCATAGA	CCTCTTCATTCTTAGGACAGTTGGC
	Ym1	GGGCATACCTTTATCCTGAG	CCACTGAAGTCATCCATGTC
	Arg1	CAGAAGAATGGAAGAGTCAG	CAGATATGCAGGGAGTCACC
House-keeping	*Beta-actin*	TGGAATCCTGTGGCATCCATGAAAC	TAAAACGCAGCTCAGTAACAGTCCG

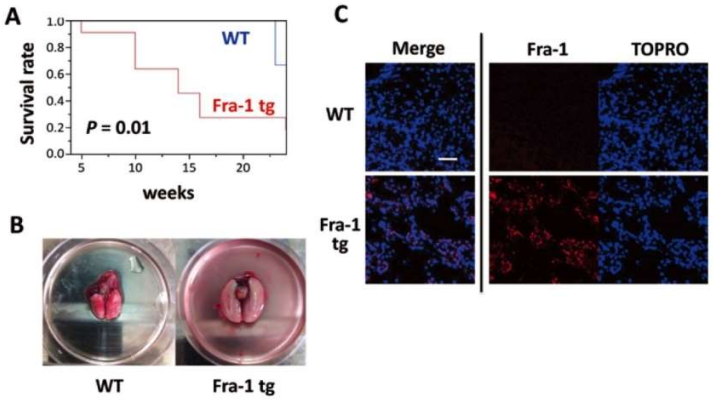

Supplemental Figure 1. Survival of constitutive Fra-1 transgenic (tg) mice (A) Survival rates of 11 pairs of Fra-1 tg and wild-type (WT) littermate mice. (B) Macroscopic images of the cardiovascular system, including the lungs and heart, of WT and Fra-1 tg mice. (C) Expression of Fra-1 (red) in lung tissue from constitutive Fra-1 tg mice and WT littermates. Nuclei were counter-stained with TO-PRO3 (blue). Bar denotes 100 µm.

508x677mm (72 x 72 DPI)

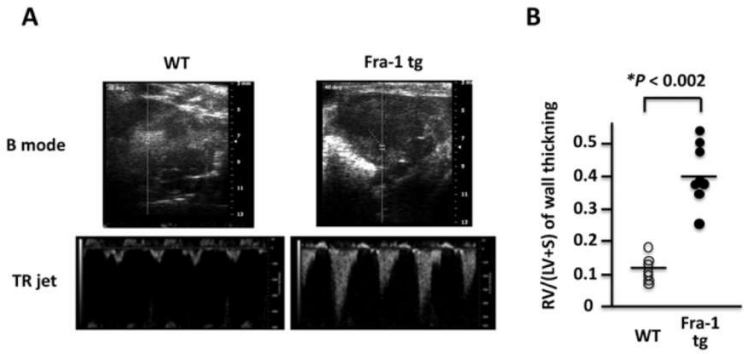

Supplemental Figure 2. Evaluation of pulmonary circulation in Fra-1 transgenic (tg) mice.
(A) Representative result of transthoracic echocardiography of 10-week-old Fra-1 tg and wild-type (WT) mice. Upper panels show B mode images and lower panels show Doppler images used to measure the jet of tricuspid regurgitation (TR). (B) Ratio of right ventricle wall thickening to left ventricle wall thickening plus septum thickening (RV/[LV+S]) in Fra-1 tg and WT mice. Statistical comparison was made using the Mann-Whitney U-test.

508x677mm (72 x 72 DPI)